

- dissociation energy corrected for $T = 0$ K); (b) S. W. Benson, "Thermochemical Kinetics", 2nd ed., Wiley, New York, 1976.
- (14) P. Venkateswarlu and W. Gordy, *J. Chem. Phys.*, **23**, 1200 (1955).
- (15) W. A. Lathan, L. A. Curtiss, W. J. Hehre, J. B. Lisle, and J. A. Pople, *Prog. Phys. Org. Chem.*, **11**, 175 (1974).
- (16) The electron-transfer numbers come from simple Mulliken population analyses. These numbers are not exact; the Mulliken population only indicates general trends in electron distribution.
- (17) (a) J. B. Coon, N. W. Naugle, and R. D. McKenzie, *J. Mol. Spectrosc.*, **20**, 107 (1966); (b) V. A. Job, V. Sethurama, and K. K. Innes, *ibid.*, **36**, 365 (1969); (c) R. B. Lawrence and M. W. P. Strandberg, *Phys. Rev.*, **83**, 363 (1951); (d) L. B. Harding and W. A. Goddard III, *J. Am. Chem. Soc.*, **97**, 6293 (1975).
- (18) E. H. von Veen, W. L. van Dijk, and H. H. Brongersma, *Chem. Phys.*, **16**, 337 (1976).
- (19) Some relevant total energies (hartrees): GVB(7/17), methanol $E = -115.17441$, sodium methoxide $E = -114.79418$; Cl, methanol $E = -115.09502$, sodium methoxide $E = -114.71685$. For the radical species of GVB(6/12): hydroxymethyl radical, -114.50432 ; sodium ketyl, -114.18503 ; Cl, hydroxymethyl radical, -114.43355 ; sodium ketyl, -114.07170 .
- (20) D. A. Evans and D. J. Baillargeon, *Tetrahedron Lett.*, 3319 (1978).

Application of *ab Initio* Molecular Orbital Calculations to the Structural Moieties of Carbohydrates. 5.¹ The Geometry of the Hydrogen Bonds

M. D. Newton,* G. A. Jeffrey, and Shozo Takagi

Contribution from the Chemistry Department, Brookhaven National Laboratory, Upton, New York 11973, and the Department of Crystallography, University of Pittsburgh, Pittsburgh, Pennsylvania 15260. Received August 13, 1978

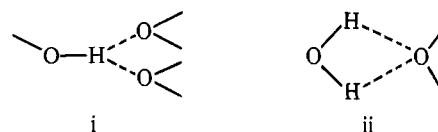
Abstract: *Ab initio* RHF/4-31G level molecular orbital calculations and Boltzmann factors are used to calculate the room temperature probability distribution of the O–H...O hydrogen-bond angle using a model consisting of two methanol molecules. The maximum in the distribution curve occurs at 163°. The data available from 18 neutron diffraction studies of carbohydrates yield a mean value of 166°. The energetics of symmetrical and asymmetrical bifurcated hydrogen bonds, which are not uncommon in carbohydrate crystal structures, were modeled with three water molecules. It is found that a symmetrical bifurcated hydrogen bond with typical geometry is more stable, relative to 3H₂O, than an equilibrium linear bond, relative to 2H₂O, by 1–2 kcal/mol. For a typical asymmetrical bifurcated geometry, the addition of a third water molecule to a "linear" bond with an O–H...O angle of 150° can lead to further stabilization of 1–4 kcal/mol, depending upon the geometry of the system.

I. Introduction

Simple monosaccharides are an excellent source of data for studying hydrogen bonding.² The molecules are approximately ellipsoidal and have an external surface which consists primarily of hydroxyl groups. Hydrogen bonding involving these groups can be expected to dominate the intermolecular cohesive forces, with other polar interactions and van der Waals forces playing only a secondary role. The molecules consist of singly bonded first-row elements and are therefore very suitable for modeling *ab initio* molecular orbital methods.³ Although concentrated carbohydrate solutions are prone to form syrups, when nucleation is induced well-formed crystals of neutron diffraction quality and size can frequently be obtained. These crystals have relatively high melting points and the thermal motion of the molecules in the crystal lattice is relatively small and isotropic for molecular weights of less than 200 consisting of first-row elements only. These factors simplify the problems of obtaining the high-precision structural data relating to the hydrogen atoms necessary to understand the structure of the hydrogen bonds.

In this paper we consider from a theoretical point of view the factors which bear on the hydrogen-bond angle (\angle OH...O) and compare our predictions with experimental data from single-crystal neutron diffraction analyses. We will address two questions: (1) What is the most probable O–H...O angle for a "linear" hydrogen bond? (We use the term "linear" in a general sense to refer to the simple open hydrogen-bonded structure, –O–H...O, and not simply to the limiting case when \angle OH...O = 180°.) (2) To what extent can departures from the most probable angle be facilitated by the involvement of

an additional proton acceptor, in a configuration which we denote as a *bifurcated* hydrogen bond (i)? This is the standard usage of the term in the crystallographic literature.⁴ Theo-



retical workers have tended to use "bifurcated" to denote a different double hydrogen-bond configuration;⁵ i.e., the type ii. Since this is never observed in carbohydrate crystal structures, we shall not consider it in the present study.

A detailed comparison of theoretical and experimental aspects of hydrogen bonding based solely on neutron diffraction data is appropriate at the present time, since there have been four recent analyses^{6–10} based primarily on X-ray diffraction results. In these X-ray data, the hydrogen positions are subject to large errors, usually in the direction of appearing closer to the covalently bound oxygen, by as much as 0.3 Å. In consequence, the O...O separations may be accurate to better than 0.005 Å, but the covalent O–H bond lengths and the hydrogen-bond H...O bond lengths can have errors as large as 0.3 Å and the O–H...O angles are subject to errors of ~5–10°.

There are now sufficient neutron diffraction crystal structure determinations of carbohydrates to permit an analysis of the geometry of the O–H...O bonds from data in which the hydrogen-atom positions are as accurately located as are those of the oxygen atoms. In general, all the bond lengths have standard deviations of 0.002–0.003 Å, and the angles of 0.3°. We shall defer discussion of the systematics which have

* Brookhaven National Laboratory.

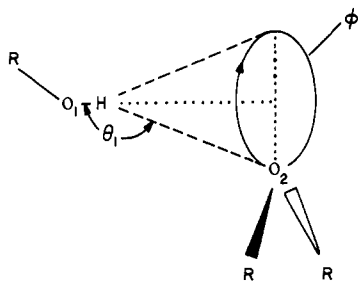


Figure 1. Schematic representation of bent OH...O hydrogen bond. The torsion angle ϕ is equivalent to angle ϕ_1 in the more detailed structure shown in Figure 2.

emerged from this data until section IV, where the present theoretical results are compared with experiment.

II. Linear Hydrogen Bonds

A. Specification of Model. At the simplest level, one might hope to understand the energetics of the hydrogen-bond angle in terms of the abbreviated structural model depicted in Figure 1. If one assumes isotropy with respect to the azimuthal angle, ϕ , and further assumes that the minimum energy corresponds to $\angle \text{O}_1\text{H}\cdots\text{O}_2 = 180^\circ$, then a simple one-parameter potential energy function suggests itself, which, when incorporated into a Boltzmann factor and modified by an appropriate Jacobian factor ($\sin \theta_1$), leads to the following temperature-dependent differential probability:

$$\bar{g}(\theta_1) \sin \theta_1 d\theta_1 = A \exp\{-(f\theta_1'^2)/(2KT)\} \sin \theta_1 d\theta_1 \quad (1)$$

where A is a normalization constant, f is the assumed harmonic bending force constant, $\theta_1' = (\theta_1 - 180^\circ)$, and K is Boltzmann's constant.

In the present study we shall take a more detailed look at the assumptions noted above and shall consider the problem from the more general framework represented by the linear (i.e., open; see section I) methanol dimer shown in Figure 2.¹¹ The six intermolecular coordinates used here are especially appropriate for comparison with neutron data, which provide accurate values for $r_{\text{H}\cdots\text{O}_2}$ and $\angle \text{O}_1\text{H}\cdots\text{O}_2$.¹²

In principle, we could calculate $\bar{g}(\theta_1)$ by performing a complete Boltzmann average over the four remaining angles, ϕ_1 , ϕ_2 , θ_2 , and χ , and the $\text{H}\cdots\text{O}_2$ distance, r . In the following we develop a simpler approach and attempt to understand the degree to which the approximate expression in eq 1 can be justified.

Selection of Values for r , θ_2 , and χ . Our first approximation is to employ average values for r , θ_2 , and χ , since analysis of the neutron data² given in section IV indicates that (1) these parameters are only weakly correlated with the parameter of primary interest, θ_1 , and (2) the observed values are reasonably well clustered about their mean values.

The value adopted for r is 1.94 Å.^{2a} It is close to the optimal value (1.99 Å) yielded by an SCF MO calculation for the methanol dimer (6-31G* basis)^{3c} and is based on a sample of 17 neutron and corrected X-ray data points corresponding to hydrogen-bonded carbohydrate OH groups, where the proton donor OH group is not also serving as an acceptor for another OH group.^{2a} This type of bonding corresponds most closely to our dimer model. The values of r tend to be appreciably smaller when the donor OH group also serves as a proton acceptor.^{2a,3b} At first glance, the use of a fixed r might seem questionable, since correlations between θ_1 and r have been postulated.⁷ However, these correlations were on a large sample of both X-ray and neutron data, which included very strong and very weak H bonds. As we will show later, the correlation between r and θ_1 is so small for the range of OH...O

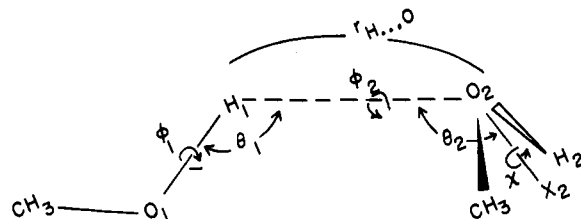


Figure 2. Methanol dimer geometry. The torsional angles ϕ_1 , ϕ_2 , and χ are defined by the sequences C-O₁-H₁-O₂, X₂-O₂-H₁-O₁, and C-O₂-X₂-H₁, respectively (O₂-X₂ bisects the CO₂H₂ angle, X being a dummy atom), and are governed by the conventions introduced by Klyne and Prelog.²⁵ The arrows (\curvearrowright) show the sense of rotation of the vectors C-O₁, X₂-O₂, and C-O₂ associated with increasing the values of ϕ_1 , ϕ_2 , and χ , respectively. The figure corresponds to $\phi_1 = 180^\circ$, $\phi_2 = 0^\circ$, $\chi = 90^\circ$.

bonds spanned by the carbohydrate neutron data ($r = 1.70$ - 2.0 Å) that it is barely observable from the experimental data. Accordingly, our use of an average value is appropriate for studying the angle dependence of these hydrogen bonds of moderate strength.

The value of 132° adopted for θ_2 is the optimal value obtained from SCF MO dimer calculations (6-31G* basis)^{3c} and is close to the average value of 139° exhibited by a set of 12 typical hydrogen bonds (neutron data).¹³ The average deviation from the mean is 12° (maximum, 38°). Finally, we consider the torsional angle χ . From consideration of lone-pair directionality in the proton acceptor molecule, we expect energetically accessible χ values to be clustered close to $\pm 90^\circ$. Del Bene found $\chi = 85^\circ$ for the equilibrium structure of the methanol dimer, based on STO-3G MO calculations.¹⁴ The sample of 12 H bonds discussed in the previous paragraph shows that the average departure of χ from either $+90^\circ$ or -90° is only 15° (maximum, 33°). Accordingly, χ is restricted to $\pm 90^\circ$ in the averaging defined below.

Sampling of the Torsion Angles, ϕ_1 and ϕ_2 . In contrast to the parameters just considered, the values of ϕ_1 and ϕ_2 in the sample of 12 hydrogen bonds effectively span the entire possible range ($0 \rightarrow 2\pi$). This is consistent with the fact that ab initio calculations carried out in the present study (see below) yielded many different energetically favorable ϕ_1 , ϕ_2 values. Accordingly, the whole range of ϕ_1 and ϕ_2 was included in our averaging procedure through the use of a crude grid ($0, \pm 90, 180^\circ$). It should be noted that in the limit, $\theta_1 = 180^\circ$, only one independent torsion angle, ϕ , survives, and we associate it with the sequence X-O₂-O₁-C in Figure 2.

Distribution Function. We can now write a generalized differential probability function.

$$g(\theta_1, r, \theta_2, \chi, \phi_1, \phi_2) \sin \theta_1 d\tau = A' \exp\{-V(\theta_1, r, \theta_2, \chi, \phi_1, \phi_2)/KT\} \sin \theta_1 d\tau \quad (2)$$

where A' is an arbitrary normalization constant (cf. eq 1), V is the potential energy, and $d\tau$ is the product of differentials of each of the parameters which are varied in the present model (i.e., θ_1 , χ , ϕ_1 , ϕ_2). By averaging over χ , ϕ_1 , and ϕ_2 , using appropriate values of V , we can generate the analogue of the assumed relation, eq 1. However, in order to test the assumption of isotropy implicit in eq 1, it is useful first to consider

$$\bar{g}(\theta_1, \phi_1) \sin \theta_1 d\theta_1 d\phi_1 = \sum_{\substack{\chi=\pm 90^\circ \\ \phi_2=0, \pm 90, 180^\circ}} g(\theta_1, \chi, \phi_1, \phi_2) \sin \theta_1 d\theta_1 d\phi_1 \quad (3)$$

where the parameters r and θ_2 , which are kept at their fixed average values, have been suppressed. The averaging is performed over ϕ_2 and not ϕ_1 , so as to allow close correspondence with Figure 1, in which ϕ is clearly equivalent to ϕ_1 . At this

Table I. Calculated Values of \bar{g} , \bar{g} , and \bar{P}

θ_1 , deg	$\bar{g}(\theta_1, \phi_1)^{a,b}$			$\bar{g}(\theta_1)^{b,c}$	$\bar{P}(\theta_1)^d$
	$\phi_1: 0^\circ$	$\pm 90^\circ$	180°		
180	← 1.000 ^e →			1.000	0.000
172.5	0.930	0.908	0.886	0.908	0.119
165	0.684	0.683	0.660	0.678	0.175
157.5	0.379	0.419	0.409	0.407	0.156

^a Defined by eq 3. ^b Normalized to unity for $\theta_1 = 180^\circ$. ^c Defined by eq 4. ^d Based on eq 4. The most probable value of θ_1 is 163.2° ($\bar{P} = 0.176$), based on interpolation of the data. ^e ϕ_1 not defined for $\theta_1 = 180^\circ$.

point, we must specify a means of evaluating V . We have adopted SCF MO theory in the 4-31G level.¹⁵ This level has been very useful in modeling a number of structural aspects of carbohydrate chemistry, including conformational and hydrogen-bonding phenomena.^{16,3b,3c}

B. Results. The calculated values of $\bar{g}(\theta_1, \phi_1)$ are displayed in Table I, for a grid of the polar angles, θ_1 and ϕ_1 . For $\theta_1 = 180^\circ$, only a single entry is given since ϕ_1 is undefined. It is apparent that, for a given value of θ_1 , $\bar{g}(\theta_1, \phi_1)$ is roughly independent of ϕ_1 , and our calculations thus give numerical justification to the notion of isotropy with respect to the torsional motion represented by ϕ in Figure 1 (recall that this ϕ is equivalent to ϕ_1 of Figure 2). Detailed examination of the calculated energies shows that the invariance of \bar{g} with respect to ϕ_1 arises from the fact that $V(\theta_1, \phi_1, \phi_2)$ attains a nearly constant minimum value when the relation $\phi_1 + \phi_2 = 180^\circ$ is maintained. Of course, this relationship was only verified for the grid of values defined above ($0, \pm 90, 180^\circ$). It should also be noted that only 3 out of 11 cases from the sample of neutron data¹³ came close to following the above ϕ_1, ϕ_2 correlation (the 12th case has $\theta_1 = 180^\circ$; hence there is only one torsion angle, ϕ , as noted above). Nevertheless, the calculations indicate that the observed ϕ_1, ϕ_2 values in the remaining eight cases should be energetically accessible, since they correspond to energies within 1–2 kcal/mol of the minimum energy structure ($\theta_1 = 180^\circ, \phi = 180^\circ$).

Averaging of $\bar{g}(\theta_1, \phi_1)$ over ϕ_1 (of minor numerical significance in view of the near invariance) and multiplication by $\sin \theta_1$ yields the (unnormalized) probability function

$$\bar{P}(\theta_1) = \bar{g}(\theta_1) \sin \theta_1 = \sum_{\phi_1=0, \pm 90, 180^\circ} \bar{g}(\theta_1, \phi_1) \sin \theta_1 \quad (4)$$

which is included in Table I and plotted in Figure 3, revealing a most probable value of θ_1 near 163° . The data of Table I and Figure 3 are compared with experiment in section IV. For completeness we note that averaging of g over ϕ_1 instead of ϕ_2 (as in eq 3) yields a function which depends rather strongly on ϕ_2 , in contrast to the situation for $\bar{g}(\theta_1, \phi_1)$.

We can now employ our calculated values of $\bar{g}(\theta_1)$ to obtain a value for the effective force constant, f , which appears in eq 1. A least-squares fit of $-(KT) \ln \bar{g}(\theta_1)$ to a quadratic function of θ_1 (using the data of Table I) yields

$$V(\theta_1) = (2.2 \times 10^{-3})(\theta_1 - 180^\circ)^2/2 \quad (5)$$

where V is in kcal/mol and the range of θ_1 is 0 – 180° . The finding of a minimum at 180° was not constrained, but was a result of the least-squares criterion (to within $\sim 0.1^\circ$). The derived effective force constant (2.2×10^{-3} kcal/(mol deg²)) is $\sim 5\%$ of typical bending force constants for single covalent bonds and indicates the softness of the hydrogen bond potential energy with respect to bending.¹⁷

The closeness of the equilibrium value of θ_1 to 180° also emerged in a more direct fashion from the ab initio calculations. Thus, values of 178.0 and 177.1° were obtained when ϕ_1, ϕ_2 were given the values $180, 0$ and $90, 90^\circ$, respectively.

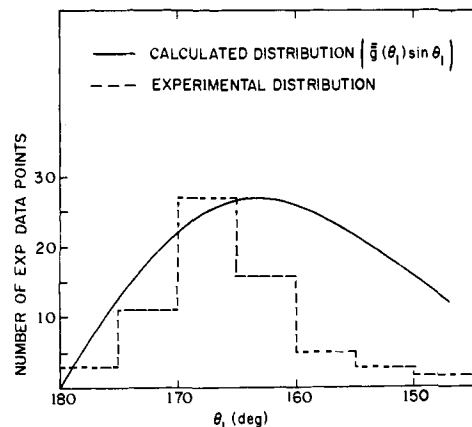


Figure 3. Comparison of theoretical (solid smooth curve, eq 4, peaking at 163°) and experimental (dashed histogram, peaking at 165 – 170°) θ_1 distribution functions. The mean value of the experimental data is 166° . The height of the theoretical curve is arbitrary and is drawn so as to have the peak heights of the two curves coincide.

The corresponding quadratic force constants were found to be 1.94×10^{-3} and 2.19×10^{-3} kcal/(mol deg²). The important point to note is that there is no unique bending force constant, since there are two linearly independent bending motions, irrespective of the value of θ_1 . Once again, however, the numerical results show near isotropy, since the two force constants listed above are similar in magnitude and are also close in value to the effective force constant associated with eq 4 and 5.

As a final comment, we note that the equilibrium values of $r_{H_1 \dots O_2}$ calculated for θ_1 at 180 and 165° differed by only 0.007 Å (1.882 and 1.889 Å, respectively), thus confirming our earlier assumption that r and θ are not strongly coupled. (These calculations were based on $\phi_1, \phi_2 = 180, 0^\circ$, these being the lowest energy values for $\theta_1 \neq 180^\circ$; for $\theta_1 = 180^\circ$, ϕ was set equal to 180° .)

III. Bifurcated Hydrogen Bonds

The previous discussion indicates that at room temperature the most probable angle in a "linear" hydrogen bond will be $\sim 165^\circ$. Appreciably larger deviations from $\sim 180^\circ$ will become costly in energy; e.g., the minimum-energy¹⁸ configurations associated with $\theta_1 = 150$ and 135° are calculated to lie ~ 0.8 and 2.1 kcal/mol, respectively, above the energy of the $\theta_1 = 180^\circ$ structure ($KT = 0.592$ kcal/mol at room temperature). However, as θ_1 decreases, the donated proton becomes increasingly accessible to additional proton-acceptor molecules, since, by virtue of the bond bending, the heavy atoms of the proton-acceptor molecules can avoid contact within their van der Waals radii. Accordingly, in anticipation of our discussion of experimental data in section IV, we have calculated and compared the energies of a few linear and bifurcated hydrogen bonds, so as to understand the degree to which two proton acceptors can offset the effects of angle strain. The bifurcated trimer structure is depicted in Figure 4. The trimer calculations were based on water molecules¹⁹ for reasons of economy in computing. Similar results would be expected for methanol. In the calculations, certain parameters were fixed ($\chi_2, \chi_3 = 90^\circ, \theta_2, \theta_3 = 132^\circ$) and various values of $\phi_1, \theta_1, \theta_1', \phi_2$, and ϕ_3 and the two $H_1 \dots O$ distances were considered. Inspection of experimental data² suggested two general situations of interest: the symmetric case ($\theta_1 = \theta_1'; r_{H_1 \dots O_2} = r_{H_1 \dots O_3}$) and the strongly asymmetric case, which is best described as a bent linear hydrogen bond perturbed by an additional long-range bent hydrogen bond. In both cases, H_1 and the three oxygen atoms are nearly coplanar, and coplanarity was assumed in the calculations, the results of which are summarized in Table II. The

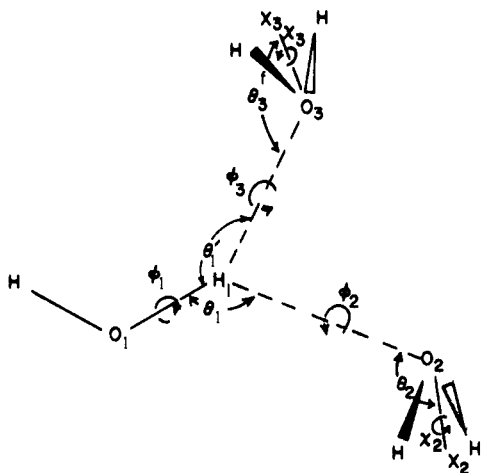


Figure 4. Water trimer with bifurcated hydrogen bond. Angles are defined analogously to those in Figure 2. As drawn, the figure corresponds to $\varphi_1 = 180^\circ$, $\varphi_2 = 0^\circ$, $\varphi_3 = 0^\circ$; $\chi_2 = \chi_3 = 90^\circ$.

Table II. Energies of the Bifurcated Hydrogen Bonds in Water Trimers^a

φ_1 , deg	φ_2 , deg	φ_3 , deg	E_{rel}^b	
			trimer	ref dimer
180	A. Symmetric Oxygen Framework ^c			
	0	180	-10.3	-8.0 ^d
		± 90	-8.8	
180	B. Asymmetric Oxygen Framework ^e			
	0	180	-10.9	-7.10 ^f
		± 90	-9.1	
		0	-7.9	

^a Structural parameters are defined in Figure 4. ^b Energy (kcal/mol) relative to separated monomers. ^c $r_{H_1 \dots O} = 2.15 \text{ \AA}$, $\theta_1 = 135^\circ$. ^d Energy of linear dimer ($\theta_1 = 180^\circ$; torsion angle $\angle X_2-O_2-O_1-H = 180^\circ$; other parameters the same as in trimer calculations). ^e $r_{H_1 \dots O_2} = 1.95 \text{ \AA}$, $r_{H_1 \dots O_3} = 2.50 \text{ \AA}$, $\theta_1 = 150^\circ$, $\theta_1' = 110^\circ$. ^f Energy of dimer obtained by removing third water molecule (O_3) from asymmetric trimer, keeping other parameters fixed.

tabulated energies are relative to the separated monomers, and the entries in the last column refer to "linear" dimer structures, with the third monomer at infinite separation. The data included correspond to those choices of φ_1 , φ_2 , and φ_3 (0, ± 90 , or 180°) for which the stabilization of the bifurcated trimer (relative to $3H_2O$) is at least as great as that for the "linear" dimer (relative to $2H_2O$).

For the symmetric case (Table IIA), the specification of the framework geometry was completed by assigning typical experimental values,² $\theta_1 = 135^\circ$ and $r_{H \dots O} = 2.15 \text{ \AA}$ (subsequent optimization²⁰ of the calculated values yielded 132° and 2.22 \AA). The symmetric bifurcated bond is seen to be more stable than an equilibrium linear dimer by $\sim 1\text{--}2 \text{ kcal/mol}$.²¹

For the asymmetric model the fixed parameters were set at $r_{H_1 \dots O_2} = 1.95 \text{ \AA}$, $r_{H_1 \dots O_3} = 2.50 \text{ \AA}$, $\theta_1 = 150^\circ$, and $\theta_1' = 110^\circ$. We find (Table IIB) that addition of a third water molecule (O_3) to the bent ($\theta_1 = 150^\circ$) "linear" hydrogen bond ($O_1-H_1 \dots O_2$) leads to appreciable further stabilization ($\sim 1\text{--}4 \text{ kcal/mol}$, depending on φ_3).²¹

Thus, while the bifurcated hydrogen bond does not appear to be twice as stable as a normal linear hydrogen bond, it does nevertheless constitute an energetically favorable interaction in both the symmetric and asymmetric cases, and provides a mechanism which more than compensates for energy costs associated with strongly bent hydrogen bonds. As in the case of linear hydrogen bonds, the bifurcated interaction would be expected to be enhanced if the acceptor oxygen atoms also

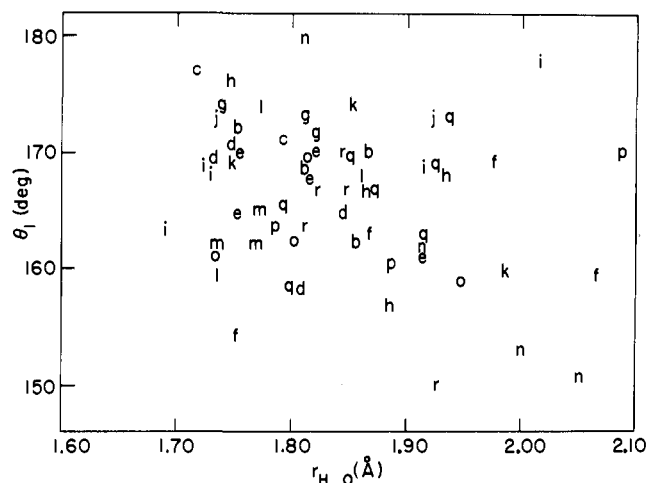


Figure 5. Plot of O-H...O angle vs. H...O distance, based on 65 neutron diffraction data points (two other points are off-scale). The letters a through r identify the 18 carbohydrates from which the data are taken.²²

serve as proton donors.^{2a,3b}

IV. Comparison with Experimental Data

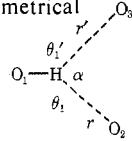
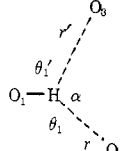
Figure 5 shows a plot of hydrogen-bond distance against hydrogen-bond angle for the "linear" hydrogen bonds observed in the 18 neutron diffraction analyses of the simple mono- and disaccharides that constitute the experimental data base for this study.²² No distinction was observed between hydroxyl groups which were both donors and acceptors and those which were donors only, and both are included in the plot. Nor was there any basis for separating the hydrogen bonds with hydroxyl and acetal or hemiacetal oxygens as acceptors. Within the range of H...O distances observed in these structures, a correlation between H...O distances and O-H...O angle is barely observable,²³ in agreement with the theoretical conclusion that r and θ are very weakly coupled.

The plot of the experimental distribution of hydrogen-bond angles is shown in Figure 3. The 67 observations were grouped into 5° angular ranges so the statistics are not especially good. There appears to be a trend for the observed angle distribution to be narrower than the theoretical and to peak at a few degrees above the theoretical value of 163° . The mean value of the experimental values is 166° .

The neutron data on the symmetrical and asymmetrical bifurcated hydrogen bonds are given in Table III. These bonds were identified by examining the 18 crystal structures²² for nearest-neighbor oxygen atoms in the direction of the bisector of the O-H...O angle of the shorter H...O bond in those cases where the O-H...O angle was less than the expected value of $\sim 165^\circ$. Of the 79 hydrogen-bond interactions observed in the 18 structures examined, an appreciable fraction ($\sim 15\%$) are of the bifurcated type, which is consistent with the theoretical prediction that bifurcated bonding involves energies comparable to those of normal linear bonds. When an oxygen atom was found at a distance of less than 2.8 \AA (i.e., $r_{H_1 \dots O_3} < 2.8 \text{ \AA}$, Figure 3), the data were excluded from Figures 3 and 5 and placed in Table III.

Figure 6 shows the correlation between the covalent O-H bond lengths and the hydrogen bond length. Here there is evidence of a weak relationship, going from 0.98 \AA for a short H...O hydrogen bond of 1.60 \AA to 0.96 \AA for a long hydrogen bond of 2.0 \AA . It is important, however, to realize that there is no experimental evidence from these diffraction data that this relationship is a consequence of any changes in the electronic structure of the molecules at rest. In the crystal structures, the hydrogen bonding affects the thermal motion of the

Table III. Geometry of Bifurcated Bonds^a

	θ_1 , deg	θ_1' , deg	r , Å	r' , Å	α , deg	ref ^b
symmetrical						
	117	135	2.138	2.185	98	22j
	130	140	2.085	2.140	89	22j
	136	141	2.151 ^d	2.209 ^d	81	22h
	146	123	2.112 ^e	2.634 ^e	91	22c
asymmetrical						
	152	104	1.965	2.349	92	22f
	169	114	1.977	2.593	75	22f
	149	120	1.949	2.715	120	22g
	147	107	1.957	2.300 ^c	106	22c
	163	120	1.953	2.582	73	22h
	139	96	1.958 ^c	2.568	125	22o
	147	135	1.989	2.495	77	22o
	139	90	1.947	2.696	111	22o

^a In sucrose,²² there is a trifurcated hydrogen bond with H...O distances of 2.309, 2.534, and 2.539 Å, with φ angles of 117, 103, and 152°. ^b Letters refer to data key.²² ^c Intramolecular. ^d This interaction occurs in the minor component (37%) of a crystal structure where the primary alcohol group of a ketopyranose molecule is disordered. The major component forms a linear hydrogen bond with a H...O distance of 1.867 Å and a OH...O angle of 167°. ^e This interaction might more properly be designated as asymmetrical, but is included in the symmetric group since both r values are greater than 2.00 Å, as is characteristic of the more nearly symmetric cases.

hydrogen atom, which rides on the oxygen atom to which it is attached. This riding motion results in a foreshortening artifact in the O-H bond length of a magnitude which could account for the observed trend shown in Figure 6. Unfortunately, the presently available methods of bond length corrections for thermal motion, which are based on the assumption of harmonic librations and oscillations, are inadequate to deal with this problem.

There appears to be good evidence that shorter hydrogen-bond lengths correspond to longer covalent bonds for very strong hydrogen bonds, i.e., with distances of 1.20–1.60 Å,²⁴ but for the bonds greater than 1.60 Å observed between hydroxyl groups, and between hydroxyls and acetal oxygens in carbohydrates, there is no direct evidence that this is other than a thermal motion effect.

V. Conclusions

Although the theoretical and experimental results described refer particularly to carbohydrate molecules in the crystalline state, we believe that the following conclusions will apply to the O...H-O hydrogen bonding between any polyhydric molecules, as well as water and simple alcohols.

1. Despite the fact that the equilibrium O-H...O angles are very close to 180°, the most probable angle observed at room temperature is about 165°.

2. The energetic isotropy with respect to bending the hydrogen bond is demonstrated by the calculation of nearly equal values for the two linearly independent bending force constants involved in a O-H...O bond.

3. Within the region of H...O bond distances from 1.70 to 2.00 Å, the correlation between H...O distance and O-H...O angle is small and barely observable if bifurcated bonds are excluded.

4. Where O-H...O angles of less than 160° are observed, a third oxygen is generally included in the hydrogen bonding so as to form a symmetrical or unsymmetrical bifurcated hydrogen bond of energy comparable to that of a simple linear hydrogen bond.

5. Bifurcated hydrogen bonding can therefore be expected

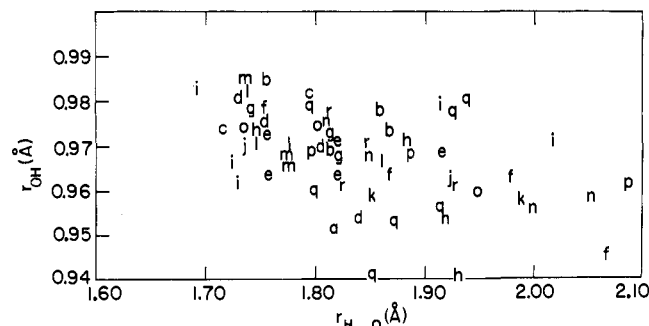


Figure 6. Plot of O-H distance vs. H...O distance, based on 64 neutron diffraction data points (three other points are off-scale). The letters have the same meaning as in Figure 5.

to occur to a significant degree in condensed phases of polyhydric molecules. About 15% of the hydrogen bonds contained in the neutron data²² discussed herein are of the bifurcated type.

Acknowledgments. This work was carried out and partially supported at Brookhaven National Laboratory under the auspices of the U.S. Energy Research and Development Administration. It was also supported in part by National Institutes of Health Grants GM-11293 and GM-21794. We gratefully acknowledge stimulating discussions with Professor L. C. Allen.

References and Notes

- For parts 3 and 4 of this series, see ref 3a.
- (a) G. A. Jeffrey and S. Takagi, *Acc. Chem. Res.*, **11**, 264 (1978). (b) Some of the neutron data is displayed in the present work in Table IV and in Figures 3, 5, and 6.
- (a) Cf. G. A. Jeffrey, J. A. Pople, J. S. Binkley, and S. Vishveshawa, *J. Am. Chem. Soc.*, **100**, 373 (1978); G. A. Jeffrey and J. Yates, *ibid.*, in press. (b) Y.-C. Tse and M. D. Newton, *ibid.*, **99**, 611 (1977). (c) A study of hydrogen-bonded dimers of water, methanol, and dimethyl ether, comparing results from STO-3G, 4-31G, and 6-31G* basis sets, has been carried out: Y.-C. Tse, M. D. Newton, and L. C. Allen, to be published.
- One of the first, if not the first, references to a bifurcated or "shared" hydrogen bond appears in the early X-ray structure analysis of glycine: G. Albrecht and R. B. Corey, *J. Am. Chem. Soc.*, **61**, 1103 (1939). Subsequent reinvestigation by neutron diffraction (P.-G. Jonsson and A. Kvick, *Acta Crystallogr., Sect. B*, **28**, 1827 (1972)) showed that the two H...O distances were 2.121 and 2.365 Å. The first definitive evidence of a symmetrical bifurcated deuterium bond was provided by the neutron diffraction analysis of perdeuterated violuric acid monohydrate: B. M. Craven and W. J. Takei, *Acta Crystallogr.*, **17**, 415 (1964). Other examples are quoted in W. C. Hamilton and J. A. Ibers, "Hydrogen Bonding in Solids", W. A. Benjamin, New York, 1968.
- (a) P. A. Kollman and L. C. Allen, *J. Chem. Phys.*, **51**, 3286 (1969); R. C. Kerns and L. C. Allen, *J. Am. Chem. Soc.*, submitted; (b) H. Umeyama and K. Morokuma, *ibid.*, **99**, 1316 (1977); K. Morokuma, *Acc. Chem. Res.*, **10**, 294 (1977); (c) M. D. Newton and S. Ehrenson, *J. Am. Chem. Soc.*, **93**, 4971 (1971).
- J. Kroon, J. A. Kanters, J. G. C. M. van Duijneveldt de Rydt, E. B. van Dureveldt, and J. A. Vliegthart, *J. Mol. Struct.*, **24**, 109–129 (1975).
- I. Olovsson and P. G. Jonsson in "The Hydrogen Bond—Recent Developments in Theory and Experiment", P. Schuster, Ed., North-Holland Publishing Co., Amsterdam, 1976, pp 395–453.
- W. A. P. Luck in ref 7, pp 529–560.
- J. Mitra and C. Ramakrishnan, *Int. J. Pept. Res.*, **9**, 27–48 (1977).
- M. Hasegawa and H. Noda, *Nature (London)*, **254**, 212 (1975).
- The use of a methanol dimer provides a more realistic model for carbohydrate hydrogen bonding than the simpler, more symmetric water dimer. The latter dimer has been employed in previous minimal-basis studies^{6,10} of OH...O angular distributions; the present methanol dimer results were obtained with the more flexible 4-31G basis.¹⁵
- (a) The coordinates used in previous theoretical studies^{4,5,6,12b,14} were generally based on the O₁...O₂ distance, which was the most reliable parameter available from X-ray^{4,6} and other^{12c} data. The study in ref 3b, however, focused on the H...O distance. (b) J. E. Del Bene and J. A. Pople, *J. Chem. Phys.*, **52**, 4858 (1970); **58**, 3605 (1973). (c) T. R. Dyke, K. M. Mack, and J. S. Muenter, *ibid.*, **66**, 498 (1977). (d) The intramolecular geometry was kept frozen at the experimental monomer values: W. Gordy and R. L. Cook, "Techniques of Organic Chemistry", Vol. IX, Part 2, 2nd ed., A. Weissberger, Ed., Interscience, New York, 1970.
- These hydrogen bonds are as follows: methyl α -D-mannopyranoside (n), O(2)-H...O(1), O(3)-H...O(4), O(6)-H...O(3); methyl α -D-glucopyranoside (m), O(2)-H...O(6), O(3)-H...O(2), O(6)-H...O(3); β -D-fructopyranose (f), O(2)-H...O(1), O(4)-H...O(2), O(5)-H...O(2); β -L-arabinopyranose (a), O(4)-H...O(2); methyl β -D-xylopyranoside (p), O(4)-H...O(2); maltose hydrate

- (r) O(2)-H...O(3). (Lower case letters refer to data key²².)
- (14) J. E. Del Bene, *J. Chem. Phys.*, **55**, 4633 (1971).
- (15) (a) R. Ditchfield, W. J. Hehre, and J. A. Pople, *J. Chem. Phys.*, **54**, 724 (1971). Standard molecular scaling factors were employed. (b) The calculations were carried out on a version of the GAUSSIAN 76 program (J. S. Binkley, R. Whiteside, P. C. Hariharan, R. Seeger, W. J. Hehre, W. A. Lathan, M. D. Newton, R. Ditchfield, and J. A. Pople (submitted to QCPE)).
- (16) M. D. Newton and G. A. Jeffrey, *J. Am. Chem. Soc.*, **99**, 2413 (1977).
- (17) (a) Somewhat larger force constants have been obtained previously (in units of kcal/(mol deg²)): $\sim 2.8 \times 10^{-3}$ (CNDO⁶); $\sim 3.5 \times 10^{-3}$ (minimal-basis ab initio¹⁰); $\sim 6-7 \times 10^{-3}$ (analysis of variance in X-ray data¹⁰). The present value of $\sim 2 \times 10^{-3}$ cannot be directly compared with the previous ones, however, since its definition is in terms of $r_{H...O}$ instead of $r_{O...O}$. Furthermore, some averaging and other approximations were employed in extracting the θ_1 force constant from the raw theoretical data.¹⁰ The precise meaning (i.e., definition in terms of internal coordinates) of the experimentally defined¹⁰ force constants is not clear. (b) The quadratic least-squares fit (eq 5) reproduces the relative energies (i.e., $-KT \ln \bar{q}$) at the four angles employed in the fit to within 2×10^{-3} kcal/mol (or better than 5%), and the root mean square deviation is 2.9×10^{-3} kcal/mol.
- (18) Minimized with respect to φ_1 and φ_2 (i.e., 180 and 0°, respectively), with the other parameters assigned as discussed in section II ($\chi = 90^\circ$, $\theta = 132^\circ$, and $r_{H...O} = 1.94 \text{ \AA}$).
- (19) K. Kuchitsu and Y. Morino, *Bull. Chem. Soc. Jpn.*, **38**, 814 (1965).
- (20) Based on optimal φ values ($\varphi_1 = 180^\circ$, $\varphi_2 = 0^\circ$, $\varphi_3 = 180^\circ$; Table III). Note that the term "symmetric" refers only to the oxygen framework, since in general ($\varphi_1 \neq \pm 90^\circ$, $\varphi_2 \neq \pm \varphi_3$) the monomer conformations destroy the symmetry plane which bisects the O₂H₁O₃ angle.
- (21) Distance-dependent basis set artifacts (e.g., see discussion in section I of ref 4c) may cause the stability of the bifurcated structure (relative to that of the dimer) to be slightly exaggerated (by ≤ 1 kcal/mol).
- (22) Key to experimental data follows. (a) β -L-Arabinose: S. Takagi and G. A. Jeffrey, *Acta Crystallogr.*, Sect. B, **B33**, 3033 (1977). (b) β -DL-Arabinose: S. Takagi and G. A. Jeffrey, *Acta Crystallogr.*, submitted. (c) β -D-Lyxose: S. Takagi and G. A. Jeffrey, *ibid.*, submitted. (d) α -L-Xylose: S. Takagi and G. A. Jeffrey, *ibid.*, submitted. (e) α -D-Glucose: G. M. Brown and H. A. Levy, *Science*, **147**, 1038 (1965). (f) β -D-Fructose: S. Takagi and G. A. Jeffrey, *Acta Crystallogr.*, Sect. B, **33**, 3510 (1977). (g) α -L-Rhamnose: S. Takagi and G. A. Jeffrey, *ibid.*, in press. (h) α -L-Sorbose: S. Nordenson, S. Takagi, and G. A. Jeffrey, *Acta Crystallogr.*, submitted. (i) D-Glucitol: Young Ja Park, G. A. Jeffrey, and W. C. Hamilton, *Acta Crystallogr.*, Sect. B, **27**, 2393 (1971). (j) Methyl α -D-altroside: B. J. Poppleton, G. A. Jeffrey, and G. J. B. Williams, *ibid.*, **31**, 2400 (1975). (k) Methyl α -D-galactoside: S. Takagi and G. A. Jeffrey, *Acta Crystallogr.*, submitted. (l) Methyl β -D-galactoside: S. Takagi and G. A. Jeffrey, *ibid.*, submitted. (m) Methyl α -D-glucoside: G. A. Jeffrey, R.K. McMullan, and S. Takagi, *Acta Crystallogr.*, Sect. B, **33**, 728 (1977). (n) Methyl α -D-mannoside: G. A. Jeffrey, R. K. McMullan, and S. Takagi, *ibid.*, **33**, 728 (1977). (o) Methyl β -D-riboside: V. J. James, J. D. Stevens, and F. H. Moore, *ibid.*, **34**, 188 (1978). (p) Methyl β -D-xyloside: S. Takagi and G. A. Jeffrey, *ibid.*, **33**, 3033 (1977). (q) Sucrose: G. M. Brown and H. A. Levy, *ibid.*, **29**, 790 (1973). (r) β -Maltose hydrate: M. E. Gress and G. A. Jeffrey, *ibid.*, **33**, 2490 (1977).
- (23) In spite of the large scatter in the data of Figure 5, a linear least-squares analysis of the 67 data points revealed a small negative slope ($\sim -20^\circ/\text{\AA}$). A similar scatter and small negative slope are apparent from Figure 8.7 of ref 7. We note that the root mean square deviation of the present fit ($\pm 6^\circ$) is slightly larger than the change in angle ($\sim 5^\circ$) predicted within the region of interest ($r_{H...O} \sim 1.7-2.0 \text{ \AA}$), thus underscoring the weakness of the coupling of angle and distance. It is also worth noting that inclusion of the eight data points which are associated with asymmetrical bifurcated interactions leads to a slope of greater magnitude ($\sim -30^\circ/\text{\AA}$); the shorter H...O member in each bifurcated set was used (see Table III). As discussed in the text, these bifurcated bonds represent special cases which accordingly were excluded from the data displayed in Figures 3, 5, and 6.
- (24) M. D. Newton, *J. Chem. Phys.*, **67**, 5535 (1977), and data cited therein.
- (25) W. Klyne and V. Prelog, *Experientia*, **16**, 521 (1960).

Investigation of the Basis of the Valence Shell Electron Pair Repulsion Model by ab Initio Calculation of Geometry Variations in a Series of Tetrahedral and Related Molecules

Ann Schmiedekamp,^{1a} D. W. J. Cruickshank,^{1b} Steen Skaarup,^{1c} Peter Pulay,^{1d} István Hargittai,^{1e} and James E. Boggs*

Contribution from the Department of Chemistry, The University of Texas at Austin, Austin, Texas 78712. Received August 28, 1978

Abstract: Energy-optimized geometries were calculated ab initio for NH₃, NF₃, OH₂, OF₂, PH₃, PF₃, SH₂, SF₂, SO₂, SOF₂, SOH₂, SO₂H₂, HSF, SH₃⁺, NH₂⁻, NF₂⁻, and NH₄⁺ using consistent basis sets and optimization criteria. An understanding of the predictions of the valence shell electron pair repulsion (VSEPR) model was sought by a comparison of the calculated geometries and various properties of the localized bonding and lone-pair orbitals. The calculated relative sizes of bonds and lone pairs agreed very well with the VSEPR assumptions. Some apparent failures of the VSEPR model can be explained by examining the total angular space requirements of the bond and lone-pair orbitals, rather than restricting attention only to the angles formed between bonds. An extensive investigation was made of the effect of polarization functions in the basis set both on calculated geometries and on the properties of the resulting localized orbitals.

Introduction

The simple valence shell electron pair repulsion (VSEPR) model² is successfully used in explaining variations of molecular geometries in extensive classes of inorganic compounds. The model assumes that the geometry around a central atom is determined by the number of electron pairs in the valence shell of that atom. Finer details of the structure are predicted by considering that nonbonding electron pairs require more angular space than single bonds, with double bonds requiring nearly as much space as lone pairs. When this model was tested against recent experimental data on some tetrahedral and related molecules, it was found³ that most, but not all, of the geometrical variations in these systems follow readily the original predictions of the VSEPR model. Gillespie noted in his book^{2a} that "... in the series CH₄, NH₃, and H₂O the bond

angle decreases from 109.5° to 107.3° and to 104.5° as the number of non-bonding pairs increases." As is demonstrated in Figure 1 by recent experimental data,³⁻¹⁷ most analogous compound series do not entirely follow this trend.

Substitution of one of the ligands by a lone electron pair in the AX₄ molecules is accompanied indeed by a decrease in the X-A-X angle and this is well understood in terms of the VSEPR model. As a second ligand of AX₃E is replaced by another lone pair, a further decrease of the XAX bond angle would be expected to occur according to Gillespie's original statement. This is observed, however, for NH₃ and H₂O, and PH₃ and SH₂ only. For other molecule pairs with chlorine or fluorine ligands the opposite trend is realized.

For systems with double bonds to oxygen, the VSEPR model does not make predictions concerning the changes in the bond